

SCIENTIFIC REPORTS



OPEN

LC/MS analysis and deep sequencing reveal the accurate RNA composition in the HIV-1 virion

Anna Šimonová^{1,2}, Barbora Svojanovská^{1,2}, Jana Trylčová¹, Martin Hubálek¹, Ondřej Moravčík³, Martin Zavřel¹, Marcela Pávová¹, Jan Hodek¹, Jan Weber¹ , Josef Cvačka¹, Jan Pačes^{1,3,4} & Hana Cahová¹ 

The mechanism of action of various viruses has been the primary focus of many studies. Yet, the data on RNA modifications in any type of virus are scarce. Methods for the sensitive analysis of RNA modifications have been developed only recently and they have not been applied to viruses. In particular, the RNA composition of HIV-1 virions has never been determined with sufficiently exact methods. Here, we reveal that the RNA of HIV-1 virions contains surprisingly high amount of the 1-methyladenosine. We are the first to use a liquid chromatography-mass spectrometry analysis (LC/MS) of virion RNA, which we combined with m¹A profiling and deep sequencing. We found that m¹A was present in the tRNA, but not in the genomic HIV-1 RNA and the abundant 7SL RNA. We were able to calculate that an HIV-1 virion contains per 2 copies of genomic RNA and 14 copies of 7SL RNA also 770 copies of tRNA, which is approximately 10 times more than thus far expected. These new insights into the composition of the HIV-1 virion can help in future studies to identify the role of nonprimer tRNAs in retroviruses. Moreover, we present a promising new tool for studying the compositions of virions.

To date, more than 140 chemical RNA modifications are known¹. Chemical RNA modification expand the repertoire of four natural nucleosides and influence RNA structure and function. The majority has been found in highly concentrated RNA moieties such as ribosomal (rRNA) or transfer RNA (tRNA). Nevertheless, there is growing evidence that coding messenger RNA (mRNA) and regulatory RNA also contain various chemical modifications². Their existence in mRNA is complicated to be proved by common LC/MS technique but special and selective profiling or capturing techniques for various RNA modification have been developed lately. In particular, pseudouridine has been found in the mRNA thanks to the development of the selective profiling techniques Pseudo-seq³ and Ψ-seq⁴. Also, the widespread presence of 5-methylcytosine across the human transcriptome has been demonstrated by a bisulphite technique combined with deep sequencing⁵. A to I editing of the mRNA has been confirmed by Inosine chemical erasing⁶. The NAD captureSeq⁷ allowed identification of RNAs with covalently attached Nicotinamide adenine dinucleotide (NAD) at 5' end. So far, this method has enabled the detection of NAD in sRNA, and mRNA in *E. coli*⁷ and in eukaryotes^{8,9}.

The development of a profiling technique for 6-methyladenosine (m⁶A) in mRNA^{10,11} paved the way for the emerging field of epitranscriptomic. Another common epitranscriptomic mark in mRNA was supposed to be 1-methyladenosine (m¹A)^{12,13}. As well as for m⁶A detection the specific antibodies have been used to detect m¹A in the human transcriptome. The problem of immunoprecipitation methods is that they do not allow for single base resolution of particular RNA modification. The authors claimed identification of thousands of transcripts bearing m¹A in eukaryotic cells. A subsequent study indicated that the m¹A is only present in 15 sites of the mRNA, in the previously known T-loop of tRNAs, and in rRNA from HEK293T cells¹⁴. Apart from

¹Institute of Organic Chemistry and Biochemistry of the Czech Academy of Sciences, Prague, 16610, Czech Republic.

²First Faculty of Medicine, Charles University, Prague, 12108, Czech Republic. ³Institute of Molecular Genetics of the Czech Academy of Sciences, Prague, 14220, Czech Republic. ⁴University of Chemistry and Technology, Prague, 16628, Czech Republic. Correspondence and requests for materials should be addressed to H.C. (email: cahova@uochb.cas.cz)

immunoprecipitation, the authors of the later method employed two types of reverse transcriptases enabling single-base resolution.

The study of the chemical structures of RNA species such as mRNA, micro RNA and guiding RNA is hampered by their very low concentrations in cells. Therefore, we believe that viruses may represent a suitable model system for RNA modification studies because they have simple intrinsic structure and well-known molecular mechanisms.

So far, m⁶A profiling is the only applied technique for the studies of viral RNA modifications. Recently, m⁶A profiling has been used to study m⁶A in the genomic RNA of *Flaviviridae*¹⁵. In particular, the conserved regions modified by m⁶A were identified in genomic RNA of hepatitis C (HCV), dengue, Zika, yellow fever and West Nile virus. The m⁶A modulated infection by HCV and the depletion of m⁶A methyltransferases or m⁶A demethylase was found to increase or decrease the HCV particle production, respectively. A photo-crosslinking-assisted m⁶A sequencing technique was used to precisely map m⁶A editing sites on the HIV-1 genome¹⁶. The m⁶A sites were found to cluster in the HIV-1 3' untranslated region and to recruit YTHDF “reader” proteins. The m⁶A editing and the recruitment of YTHDF proteins were identified as the positive regulators of HIV-1 mRNA expression.

As new layers of RNA modifications are constantly being uncovered in the transcriptome, we can presume that other RNA modifications besides m⁶A can be employed by viruses. At first, we focused on the viral packageome of HIV-1. It was believed that HIV-1 packs in virion not only two copies of genomic RNA, but also 12–14 copies of guiding 7SL RNA^{17,18}, 8 copies of tRNA^{Lys3} that serve as primer for its reverse transcriptase^{19–21}, around 12 copies of tRNA^{Lys1,2}, around 50 copies of rather randomly packed tRNAs and some fragments of other mRNA, rRNA etc^{18,22–26}. In total, the host cell-derived RNA should comprise up to half of the virion RNA by mass^{27,28}.

To best of our knowledge, the LC/MS analysis of RNA from viral particles has not been reported yet. We isolated RNA from HIV-1 viral particles, digested it into form of nucleosides and we analysed this mixture by LC/MS system. We found surprisingly high amount of m¹A (4.1% of all adenosines - A) in the packageomic RNA that corresponded to approximately 340 1-methyladenosines (Supplementary Table S1). The tRNA molecules contain one m¹A in their sequence, what correlates to 70 positions. In the light of the emerging field of epitranscriptomics we asked the question where the rest 270 m¹A can come from and whether the genomic HIV-1 RNA or other co-packed RNA are so heavily methylated. Therefore, we prepared four deep sequencing libraries with particular focus on m¹A profiling. We found that the m¹A is present solely in tRNA and that genomic HIV-1 RNA, neither 7SL RNA do not contain this modification. Based on this results we could recalculate the ratios of genomic HIV-1 RNA, 7SL RNA and tRNAs in the virion. We concluded that the HIV-1 virion consists beside 2 copies of genomic HIV-1 RNA and 14 copies of 7SL RNA also 770 copies of tRNA. Our results suggest the role for the cellular RNA could be much more significant than expected so far, both in mechanism of viral infection and in viral replication. Our study also confirms the evidence that the m¹A modification is rather typical for tRNAs¹⁴ and it is not so widespread as it was previously described¹². We also show here that the LC/MS analysis of RNA modifications in virion in combination with deep sequencing can be used for the determination of the exact RNA composition of complex virions. The presence of specific RNA modification m¹A helped us to bring new insight into the HIV-1 virion composition. In future, this method can be applied also for studies of the composition of other viruses.

Results

LC/MS technique reveals a higher amount of m¹A in the HIV-1 packageome than expected. In order to analyse the RNA modifications in the HIV-1 virus, we firstly produced HIV-1 virus by infection of MT4 cells (Fig. 1A). We harvested the supernatant both from the infected cells and the uninfected MT4 cells, and we used the latter as the mock medium. After purification of the virions on sucrose cushion, we treated the sample by RNase and DNase to digest the nucleic acids not packed in viral particles. Then, the RNA was isolated by RNazol. The samples were precipitated using ethanol and then digested by Nuclease P1 and Alkaline Phosphatase to form nucleosides. The digested RNA was analysed using a Synapt G2 LC/MS system (Fig. 1A,B). The authenticity of the methylated nucleosides was confirmed by injection of synthetic standards, which produced the same *m/z* signal and were eluted at the same time.

Using LC/MS analysis, we observed methylated adenosines. m⁶A was present only in low amount approx. 1.1%. Surprisingly, we found quite high amount of m¹A around 4.1% of all adenosines in the packageome of the HIV-1-virus. We also searched for other known modified adenosines in the RNA digest and we were able to confirm only N⁶-threonylcarbamoyl-adenosine (t⁶A), 2'-O-methyladenosine (Am) and 2-methylthio-N⁶-threonylcarbamoyl-adenosine (mS²t⁶A) (Supplementary Figures S1, S2). Other modified adenosines were not detected by our LC/MS analysis or they were present only in traces that we could not calculate (2-methylthio-N⁶-isopentenyladenosine, N⁶-(cis-hydroxyisopentenyl)adenosine, N⁶-isopentenyladenosine, Supplementary Table S2²⁹). Analysing the synthetic standards of m⁶A, m¹A, Am and t⁶A, we were able to extrapolate their proportional representation in the digest (Supplementary Figures S1, S2, Table S3). As we did not have available standard of mS²t⁶A, we presume that the molecule has similar ionization properties as t⁶A. The packageomic RNA contains 4.1% of m¹A, 1.1% of m⁶A, 0.9% of Am, 3.2% of t⁶A and 1.5% of mS²t⁶A (rest is A).

To verify that the signals of modified nucleosides originate from RNA molecules packed in viral particles, we analyzed the medium of the uninfected cells by LC/MS analysis (Supplementary Table S4). Here, we did not detect any traces of m¹A or other modified A. Thus, we conclude that the signals of modified nucleosides in the samples prepared from supernatant of HIV-1 infected cells stem indeed from RNA molecules packed in viral particles. As the RNazol protocol only isolates oligonucleotides longer than 10 nt, we can rule out the possibility that the modified nucleoside signal originates from co-packed small molecules.

Using previously published data on the number of co-packed RNA entities in one particle (two genomic HIV-1 RNAs, 14 7SL RNAs, approx. 70 tRNAs, Fig. 1C)^{18,22,23} and previous evidence on the presence of m¹A in position 58 of the majority of tRNAs, we conclude that in RNA packed in a viral particle, 270 positions would be methylated. However, this number did not correspond to the previous estimate of approximately 70 tRNA molecules.

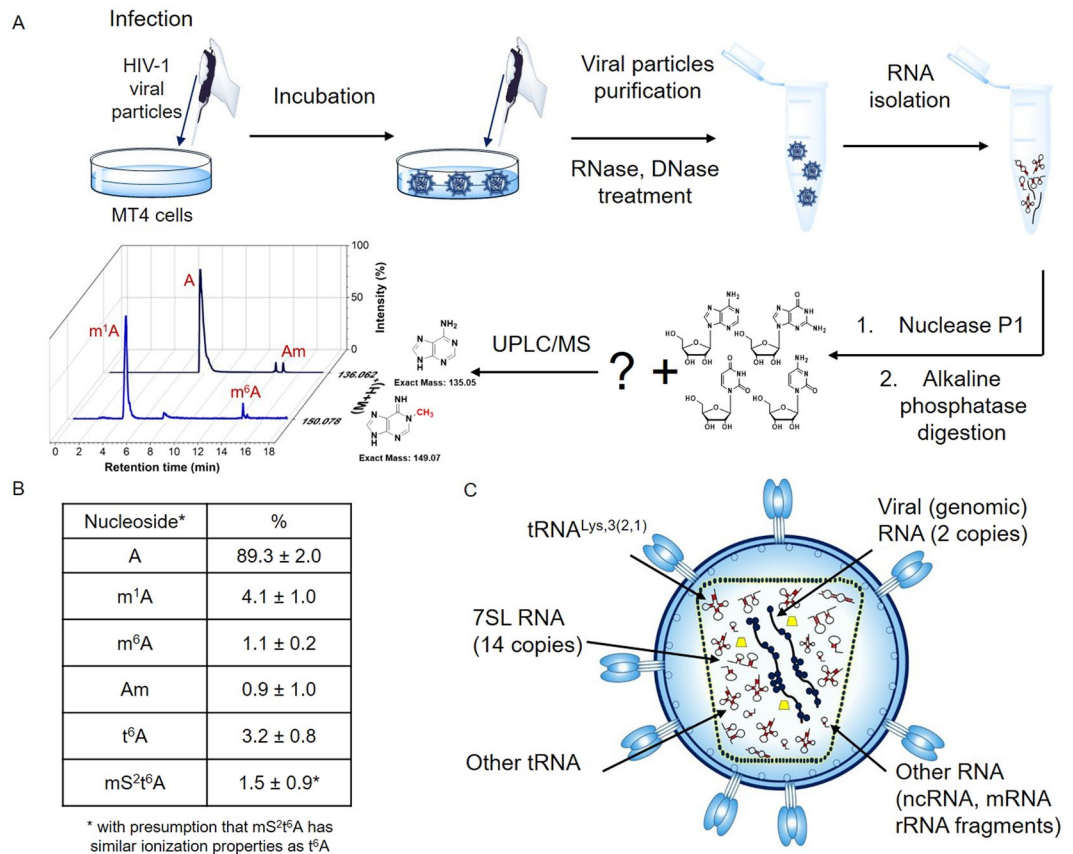


Figure 1. LC/MS analysis of RNA in the HIV-1 packageome. **(A)** Scheme showing the preparation of HIV-1 samples for LC/MS analysis. **(B)** Ratios of nucleosides in the HIV-1 samples as analysed by LC/MS using biological tetraplicates. **(C)** A schematic view on the RNA composition in HIV-1.

m¹A is solely present in the tRNA. To investigate the exact positions of m¹A in the packageomic RNA, we prepared a deep sequencing library. As the viral packageome is very simple, we used for the m¹A localisation the method based on the reverse transcription signature^{30–32}. The RNA for deep sequencing was prepared in biological triplicates. Every sample was divided in two parts and one part was treated by basic conditions to obtain an m¹A conversion to m⁶A (Dimroth rearrangement)¹² that is normally read as A by reverse transcriptase. We prepared three deep sequencing libraries using SuperScriptTM III reverse transcriptase, which should either mis-read m¹A or arrest meeting m¹A. One deep sequencing library was prepared with TGIRTTM reverse transcriptase, which should confirm the m¹A position at base resolution.

In the deep sequencing protocol (Fig. 2A), we used a sequence of the following steps: The RNA was first fragmented to obtain fragments of uniform lengths (approx. 100 nt), then ligated with the first adaptor, reverse transcribed, tailed by cytidine triphosphate (CTP) and finally ligated with the second adaptor. After PCR with indexed primers, the samples were separated using agarose gel electrophoresis. The cut off was approximately 100–350 nt including the adaptors. Afterwards, the samples were pooled in a library and sequenced by IonTorrent technology.

The bioinformatics analysis confirmed that the virion contains mainly tRNAs, 7SL RNA and HIV-1 genomic RNA (Fig. 2C, Supplementary Table S5). Any other cellular RNAs were not detected in significant amount (more than 0.1%). By analysing the deep sequencing data using bioinformatics we identified m¹A in position 58 of tRNA^{Lys} TTT-3.1, tRNA^{Lys} CTT-2.1, tRNA^{Lys} CTT-1.1, and tRNA^{Asn} GTT-2.1, as well as in position 9 of tRNA^{Asp} GTC-2.1. Based on a previous report³⁰, we expected the reverse transcriptase to be paused (observed arrest) when meeting m¹A. However, pattern of misreading for m¹A in artificial sequences read by reverse transcriptase was also reported^{30,32}. We observed this behavior of reverse transcriptase in the position 58 of some tRNAs. Approximately 70% of the m¹A in position 58^{33,34} was misread (Fig. 2B – blue colour) as G or T by both reverse transcriptases used (SuperScriptTM III – library 1–3 and TGIRTTM – library 4). In the sample that was treated with basic conditions, the misreading of position 58 was only approximately 30% (Fig. 2B). This observation corresponds to the expected conversion of m¹A to m⁶A in the RNA. It also proves the chemical authenticity of m¹A because the presence of other modified A would cause misincorporation but the ratio of misreading would not change after basic treatment.

Surprisingly, m¹A in the position 9 of tRNA^{Asp} GTC-2.1, caused rather arrest (Fig. 2B – orange colour) of SuperScriptTM III in approximately 85% and a misreading as T (86%) was observed only in the experiment with TGIRTTM. In order to verify that the m¹A profiling method works in our hand also when long RNAs are used, we tested the protocol on 28S rRNA from HEK293T cells. In this case, we observed arrest of the reverse transcriptase

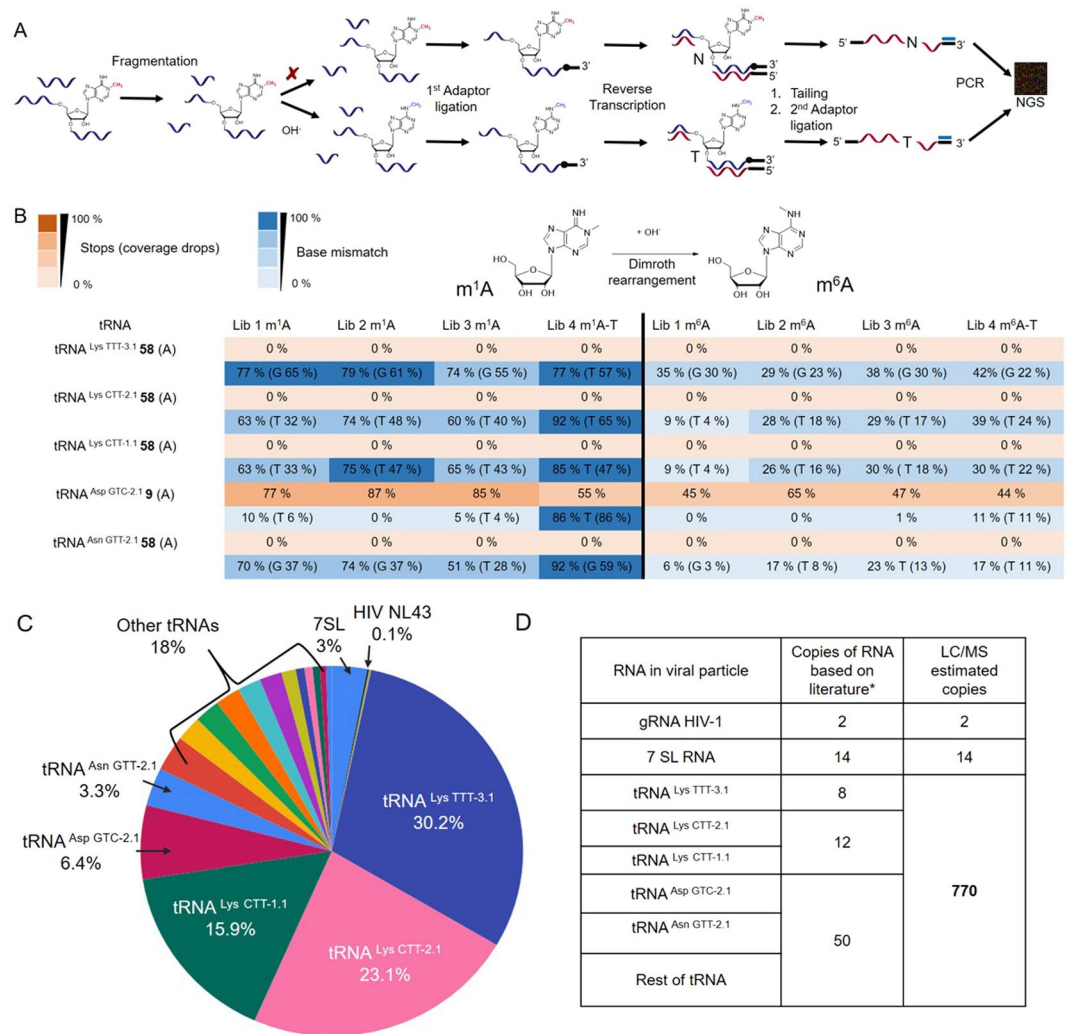


Figure 2. m¹A profiling of RNAs in HIV-1 virion. **(A)** Scheme showing the preparation of the deep sequencing libraries of RNA isolated from HIV-1 virions. **(B)** Table showing the observed misincorporation (blue) or arrests (orange) of reverse transcriptase in the deep sequencing libraries. T stands for library Lib4 prepared with TGIRT reverse transcriptase, while Lib1-Lib3 libraries were prepared with SuperScriptTM III reverse transcriptase. **(C)** The percentages of the most abundant RNA reads in the deep sequencing libraries. **(D)** Table showing the extrapolated numbers of copies of RNAs in HIV-1 virion based on literature (*)^{17,18} and on our LC/MS data.

meeting m¹A in position 1317 in 80%. This is contrary to the reverse transcriptase TGIRTTM, which misread the m¹A mainly as G in 28S rRNA (Supplementary Table S7). Our observation shows that the reverse transcriptase behavior depends strongly not only on type of RNA modification but also on sequence and 2D structure (loop, bulge etc.). In any case, the behaviour of both reverse transcriptases (either arrest or misreading) always proved the presence of m¹A.

Once we confirmed the m¹A in tRNAs co-packed in viral particle, we searched for other m¹A in all virion RNA entities. Adenosine is reported to be methylated in position 1 mainly within the specific motif GUUCNANNC¹⁴ or similar. Therefore, we looked for i) the misreading pattern, ii) the arrests of reverse transcriptase, and iii) a similar motif to GUUCNANNC (allowing one alteration) in 7SL RNA and the genomic HIV-1 RNA (Supplementary Table S7). Although we found the sequence motif allowing one alteration several times in the genomic RNA of HIV-1, we never observed a significant misreading or arresting pattern of reverse transcriptase meeting A in whole genomic RNA of HIV-1. 7SL RNA contains also one sequence motif but neither there we did not observe any significant misreading or arresting pattern. Because there are no other abundant RNA molecules beside tRNAs, (Supplementary Table S5), we concluded that all LC/MS detected m¹A originates from the co-packed tRNAs.

To exclude the possibility that the used HIV-1 particles were not sufficiently purified on the sucrose cushion and the detected RNA, thus, came from extracellular vesicles³⁵, we purified the viral particles using OptiPrep density gradient. The RNA prepared from OptiPrep density gradient purified virus represented 96% of RNA from sucrose cushion purified virus. The RNA from fractions removed by OptiPrep density gradient contained

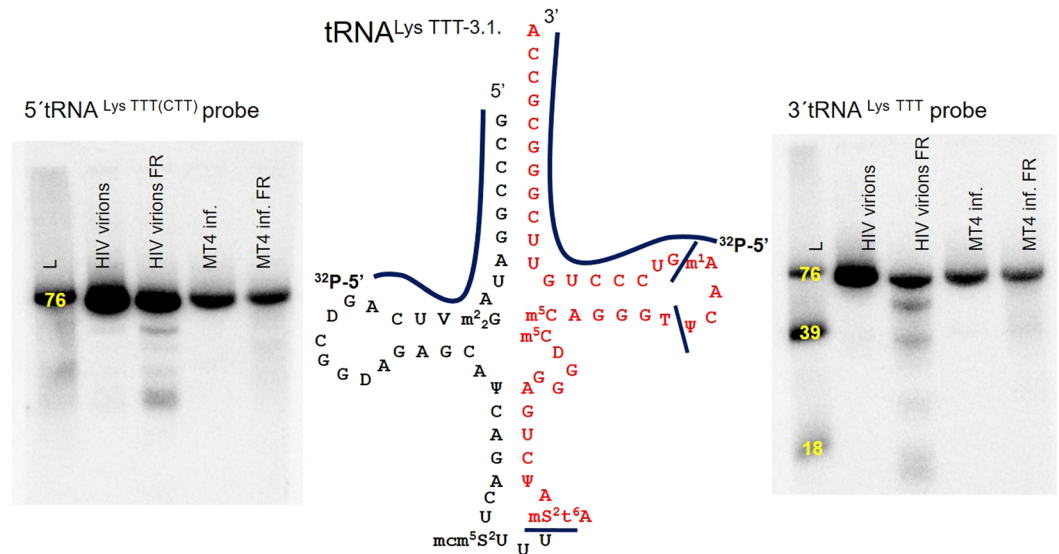


Figure 3. Northern blot analysis of RNA purified from HIV virions before and after fragmentation (FR) and from MT4 cells infected (inf.) with HIV-1 before and after fragmentation. The radioactively labelled probes were used for 5' (left panel) and 3' (right panel) ends of tRNA^{Lys TTT-3.1}. The yellow numbers stand for the size of synthetically prepared ladder (L) with the same sequence as natural tRNA^{Lys TTT-3.1}.

1000 x less HIV-1 genomic RNA (Supplementary Figure S3) and we did not observe any tRNAs using TapeStation analysis (Supplementary Figure S4A).

Based on the deep sequencing data, we can conclude that the viral particle contains more than 96% of host RNA represented mainly by tRNAs. We estimate that tRNA^{Lys TTT-3.1} is present in 30%, tRNA^{Lys CTT-2.1} in 23%, tRNA^{Lys CTT-1.1} in 16%, tRNA^{Asp GTC-2.1} in 6% and tRNA^{Asn GTT-2.1} in 3% (Fig. 2C).

Precision of mapping is in almost all cases >99% (Supplementary Figure S5). However, the determined percent was averaged over all libraries and suffer from rather high variability. We are also aware of that e.g. PCR cycles can introduce a certain bias by preferentially amplifying short sequences over long ones.

m¹A stems from full-length tRNAs. In our deep sequencing data, we only observed the 3' half of the tRNA^{Lys TTT-3.1}. We hypothesised that this phenomenon can either be explained by the presence of a bulky RNA modification such as mS²t⁶A at the anticodon loop or by the fact that the viral particle only contains the 3'-tRNA half of the tRNA^{Lys TTT-3.1}. To shed light on this, we designed a northern blot analysis of the tRNA fragments. Radioactively labelled probes were designed for the 3' ends of tRNA^{Lys TTT-3.1} and tRNA^{Lys CTT-1.1 (2.1)} as well as for the 5' end of tRNA^{Lys TTT-3.1}. As the 5' end of tRNA^{Lys TTT-3.1} and tRNA^{Lys CTT-1.1 (2.1)} is similar, the 5' end probe hybridize to all three tRNAs. We also prepared ladder with the sequence of tRNA^{Lys TTT-3.1} by *in vitro* transcription. The ladder helped us to estimate the size of observed bands. To rule out that the observed fragment in the deep sequencing data was caused by the fragmentation step, we analysed the RNA isolated from the viral particles and from the MT4 cells infected by HIV-1 before and after fragmentation. We observed the presence of 3'-tRNA fragments only in the RNA from viral particles after fragmentation (Fig. 3). Therefore, we ruled out the possibility that such 3'-tRNA fragments can contribute to the high level of m¹A. Apparently, the observed fragments were formed during the preparation of the sample and they are not naturally present in the virion. We thus conclude that m¹A solely originates from full-length tRNAs.

Nevertheless, the amount of observed m¹A did not correspond to the number of co-packed tRNAs of 70 copies total in viral particle previously published^{24–26}. Hence, we come to an end that the amount of co-packed tRNA is approximately 10-fold higher than previously reported. Based on the direct method of LC/MS analysis we can calculate that per 2 copies of genomic HIV-1 RNA and 14 copies of 7SL RNA HIV-1 virion contains also 770 copies of tRNAs (Fig. 2D, Supplementary Figure S6).

Discussion

The RNA in the packageome of the HIV-1 virus was believed to consist of 2 copies of genomic HIV-1 RNA, 14 copies of 7SL RNA and 70 copies of tRNAs. Nevertheless, so far any direct method has not been used to study the RNA composition of virions. As first, we used LC/MS to study chemical composition of packageomic RNA. Surprisingly high amount of m¹A led us to the deep sequencing analysis with particular focus on m¹A. Even though immunoprecipitation methods for mapping m¹A in complete transcriptome have been published^{12,14}, we presumed that the method based on the reverse transcription signature would be sufficient for the localisation of m¹A in simple packageome^{30,31}. m¹A profiling confirmed presence of this modification in tRNAs but excluded its presence in other RNA entities co-packed in HIV-1 virion. Once we ruled out the possibility that the m¹A can stem from tRNA fragments, we were able to recalculate ratios of RNA molecules in HIV-1 virion. Based on LC/MS analysis, we extrapolate that the virion contains per 2 molecules of genomic HIV-1 RNA and 14 copies of 7SL RNA another 770 copies of various tRNAs.

So far, only one work has dealt with a deep sequencing analysis of HIV-1 particles²⁴. According to Eckwahl *et al.*, the HIV-1 particle contain even less than 8 copies of tRNA^{Lys}^{TTT-3.1}, as was previously reported. However, Eckwahl *et al.* admit that an absence of tRNA reads in their analysis can be caused by fragmentation that would lead to fragments <50 nt. Fragmented RNA would be underrepresented in their cDNA. In our deep sequencing libraries, however, we included RNAs with a size of around 40 nt. We, therefore, did not lose those short reads. In particular, we found that tRNA^{Lys}^{TTT-3.1} caused an almost quantitative abortion of the reverse transcriptase because it contains the bulky m⁵t⁶A³⁶ in position 37. As a result, the read had a length of only 39 nt.

Our deep sequencing analysis suggests that the HIV-1 virion contains approximately 69% of three versions of tRNA^{Lys}. This is in agreement with works published by Kleiman *et al.* who found the ratio to be about 60%^{37,38}. The same group later demonstrated using both microarray and 2D Page methods that the amount of all tRNA^{Lys} is only about 45%³⁹. The reason for this difference may be imperfect labelling as both methods relied on ligation reactions.

The estimations of other co-packed tRNAs (50 molecules per virion)¹⁸ were based on the fact that the host non-coding RNAs in retroviruses outnumber viral gRNA by a factor of at least 50⁴⁰.

In other works, the quantification of further tRNAs co-packed by an HIV-1 virion was usually omitted. Based on the knowledge that every tRNA contains one m¹A in its sequence, we were able to quantify the number of all tRNAs in the viral packageome to be around 770. It is, however, important to mention that others often studied viral particles produced from different cells such as COS-7 cells^{37,38} or CEM-SS cells⁴⁰, or produced by transfection and not infection²². Those factors can influence the composition of viral particles.

A recent report on RNA modifications in viral RNA that was purified via selective probes indicates that the genomic RNA of HIV-1 can contain besides m¹A, 35 other RNA modifications⁴¹. The authors, however, conclude this fact only based on MS data, which means that the samples could be contaminated with heavily modified tRNA molecules. tRNA^{Lys}^{TTT-3.1}, for example, can be bound so tightly to gRNA that it is not possible to separate the pure genomic RNA. Another error could have been introduced in the preparation of the viral samples. As the authors used only transfection, the plasmid containing the HIV-1 genomic sequence could have been fully transcribed into RNA. Based on our screening of HIV-1 sequence, we know that the additional plasmid sequence pNL4-3 contains the original motif GUUCNANNC, which might be methylated. However, we cannot exclude that a certain position in the genomic HIV-1 is methylated from less than 5% as our profiling technique would not be able to track it. However, this amount of m¹A would not significantly contribute to the observed LC/MS signal. It is also arguable, whether such level of methylation would have any biological significance.

In our work, we also considered the existence of 3' tRNA fragments that could contribute to observed high amount of m¹A in LC/MS analysis. Pyrosequencing and recently also deep sequencing methods of small non-coding RNAs in HIV-1 infected cells have proven the existence of a very abundant 18-nt tRNA fragment from tRNA^{Lys}^{TTT-3.1} that is complementary to the HIV-1 primer binding site^{42,43}. Rather than being a primer of reverse transcription, this tRNA fragment when overexpressed led to a decrease in viral replication. Nevertheless, the concentration of these tRNA fragments was so low that we were neither able to observe the fragments in isolated RNA from infected cells nor in packageomic RNA. Other types of 3' tRNA fragments were observed only in Northern blot analysis of fragmented RNA. Therefore, we also ruled out the possibility that m¹A can come from any type of tRNA fragments.

As the role of primer tRNA^{Lys}^{TTT-3.1} is quite well understood, the function of nonprimer tRNAs such as tRNA^{Lys}^{CTT-2.1}, tRNA^{Lys}^{CTT-1.1}, tRNA^{Asp}^{GTC-2.1} or tRNA^{Asn}^{GTT-2.1} is still very enigmatic. One of the hypothesis suggests that the matrix domain of the HIV-1 Gag protein binds almost exclusively to specific tRNAs in the cytosol⁴⁴. tRNAs shield the membrane-binding surface of matrix and regulate the interaction with intracellular membranes prior reaching the plasma membrane²⁷. Cellular tRNAs might also help to import HIV-1 intracellular reverse transcription complex to nucleus⁴⁵. Another theory suggests that the enrichment of particular tRNAs in virion can manipulate with tRNA pool in cells and enhance production of the Gag polyprotein and virus production in general⁴⁶. In any case, the importance of nonprimer tRNAs in virion is very high. In this work, we bring new tool – LC/MS in combination with deep sequencing – to study the virion RNA composition. Specific RNA modifications such as m¹A can bring us missing information layer and in future, we can calculate the RNA composition of other viruses. Moreover, these techniques can be used for studies of an impact of viral infection on various RNA modification in host transcriptome.

Methods

Cell culture, transfections and infections. The human CD4 + T-cell line MT4 (NIH AIDS Reagent Program, Division of AIDS, NIAID, NIH from Dr. Douglas Richman) and the human embryonic kidney HEK293T cell line (American Type Culture Collection, LGC Standards, UK) were cultured under standard conditions at 37 °C under a humidified (>90%) atmosphere of 5% CO₂/95% air. The MT4 cell line was cultured in RPMI 1640 w/o L-Glutamine and 25 mM Hepes supplemented with 10% FBS, penicillin (100 U/mL) and streptomycin (100 µg/mL) (all Sigma-Aldrich). The HEK293T cell line was cultured in DMEM high glucose supplemented with 10% FBS, penicillin (100 U/mL) and streptomycin (100 µg/mL) (all Sigma-Aldrich).

Isolation of large and small RNA fractions from the cell culture. MT4 cells were collected by centrifugation (225 × g, 5 min, and 20 °C), HEK293T cells were collected by trypsinization and subsequent centrifugation as above. Cells pellets were washed with PBS and cells were lysed with RNazol reagent (Sigma-Aldrich). Large and small RNA fractions were purified according to the RNazol manufacturer's protocol. The RNA concentration was determined on NanoDrop ONE (ThermoFisher Scientific) and the RNA sample quality control was performed on a 4200 TapeStation System (Agilent).

Infection. MT4 cells were initially infected with a cell-free HIV-1 strain NL4-3, which was generated by transient transfection of HEK293T cells with a pNL4-3 plasmid (obtained through NIH AIDS Reagent Program, Division of AIDS, NIAID, NIH from Dr. Malcolm Martin). The infected cultures were subsequently expanded by co-cultivation. 48 h post-infection, cell culture supernatants containing viral particles and infected cells were added to uninfected MT-4 cells (5×10^5 cells per mL) at a ratio of 1:9. The co-culture was synchronized by three successive additions of infected culture supernatant to uninfected MT4 cells (5×10^5 cells per mL, the ratio of 1:9, 27 h between infections).

Virus-containing supernatants were harvested 40 h after the last synchronization step, cleared by centrifugation ($225 \times g$, 5 min, 20°C) and filtration (0.45 μm pore size cellulose-acetate filter (VWR)), and stored at -80°C .

Infectious titres were determined as 50% tissue culture infectious dose by endpoint titration using serial 10-fold dilutions of the virus on TZM-bl cells⁴⁷.

Viral particles purification and RNA isolation. *Sucrose cushion isolation.* Virus particles were concentrated from cleared culture medium by centrifugation through a cushion of 20% (wt./wt.) sucrose in phosphate-buffered saline (PBS) ($90\,000 \times g$, 90 min, 4°C). The pellet was resuspended in RNase/DNase buffer (Tris HCl 100 mM, MgCl_2 25 mM, CaCl_2 25 mM) with DNase I (10 U/mL, New England BioLabs - NEB), RNase I (200 U/mL) and RNase A (20 mg/mL, both ThermoFisher Scientific) and incubated 2 h at 37°C . RNase/DNase treatment was stopped by adding RNazol (Sigma-Aldrich).

Mock medium was prepared in the same way from uninfected MT-4 cells.

OptiPrep gradient isolation. Virus particles were concentrated and cleared through a sucrose cushion as described above. The virus pellet was resuspended in PBS, loaded to the top of the iodixanol gradient (6% to 35% OptiPrep Density Gradient medium diluted in PBS, Sigma-Aldrich) and ultracentrifuged ($90\,000 \times g$, 90 min, 4°C). HIV-containing fractions were detected by western blot analysis using the anti-HIV capsid protein antibody. Selected fractions were collected, diluted with PBS five times and the virus was pelleted by ultracentrifugation ($90\,000 \times g$, 45 min, 4°C). The virus-containing pellet was resuspended in RNase/DNase buffer and RNase/DNase treatment was performed as described above.

Western blot analysis. Samples from each fraction of the Optiprep gradient were mixed with loading buffer in the ratio of 5:1 and denatured for 5 min at 95°C . Separation was carried out at 15% SDS PAGE at constant voltage 150 V for 90 min. Separated proteins were transferred to polyvinylidene difluoride (PVDF) membrane (Bio-Rad) and blocked at casein (Blocker Casein, ThermoFisher Scientific). HIV-1 CA protein was detected with polyclonal anti HIV-1 CA antibody (sera of rabbit immunized with purified HIV-1 CA protein, produced at Institute of Physiology CAS; dilution 1:1000, 1 h, RT) and as secondary antibody was used Goat anti Rabbit IgG labelled with horseradish peroxidase (1:10000, 1 h, RT, Sigma-Aldrich). After washing, the membranes were incubated with SuperSignal West Femto Maximum Sensitivity Substrate (ThermoFisher Scientific) and the intensity of chemiluminescence was detected using the CCD camera (Las-3000, software Image Reader Las-3000, Fujifilm) (Supplementary Figure S7).

RNA from viral particles was purified by Zymo-SpinTM IIC Columns (Direct-zolTM RNA MiniPrep Plus, Zymo) according to the manufacturer's protocol. The quality of RNA samples was checked by HS RNA ScreenTape. (Supplementary Figure S4) RNA samples were quantified by an RNA High Sensitivity Assay (Quibit 4 Fluorometer, ThermoFisher Scientific), and the presence of HIV gRNA was confirmed by RT-PCR (LightCycler, Roche) (Supplementary Figure S3).

RNA digestion and LC/MS analysis. RNA samples (1–4 μg) were fully digested by Nuclease P1 (1 U/ μg of RNA, Sigma-Aldrich) in 40 μL of 50 mM ammonium acetate buffer (pH 4.5) for 1 h at 37°C . After addition of Alkaline phosphatase (CIP, 1 U/ μg of RNA, NEB) and CutSmart buffer (final concentration $1 \times$, NEB), the samples were incubated for another 1 h at 37°C . Digested RNA samples were diluted in 200 μL and purified over Microcon[®] – 10 kDa centrifugal filters (Merck). The flow-through was concentrated using a SpeedVac system to the volume of 20 μL for LC-MS analysis.

All samples were measured in technical duplicates. The separation of the digested RNA samples (8 μL injection volume) was performed by an LC system (I-Class, Waters) on a C18 column (Acquity UPLC[®] BEH C18 1.7 μm , 15 cm, Waters) at 40°C using a gradient of water (A) and acetonitrile (B), each containing 0.1% (v/v) formic acid⁴⁸. The gradient was 0–6 min, 100% A; 6–7.5 min, 100–99% A; 7.5–9.5 min, 99–94% A; 9.5–15 min, 94% A; 15–25 min, 94–50% A; 25–27 min, 50–20%; 27–29.5 min, 20% A; 29.5–30 min, 20–100% A; 30–40 min, 100% A. The flow rate was 0.05 mL/min. The autosampler cooled the samples to 8°C . The LC system was coupled on-line to a mass spectrometer (Synapt G2, Waters) to acquire masses of nucleosides by electrospray ionisation. Ions were scanned in a positive polarity mode over full-scan range of m/z 100–1200. The source parameters were as follows: capillary voltage, 3 kV; source temperature, 150°C ; sampling cone, 40; extraction cone, 5; desolvation temperature, 450°C ; desolvation gas flow, 600 L/h.

All mass chromatograms were analysed employing the MassLynx V4.1 software. Mixtures of nucleoside standards ($m^1\text{A}$, $m^6\text{A}$, Am, A, $t^6\text{A}$; Jena Bioscience, Sigma-Aldrich, CarboSynth) at three different amounts: 64, 320 and 1600 fmol each were injected on a column to compare the response of each nucleoside under defined ionization conditions. Mixtures were measured in the technical triplicates. For each standard, an extracted ion chromatogram (EIC) was generated using a major fragment observed in its full scan spectrum (fragmentation occurs in the ion source). The chromatographic peaks in EICs were integrated. The standard peak area (area under the curve, AUC) was used to calculate the ionization efficiency ratio of the tested nucleosides in this concentration range (Supplementary Table S3, Figures S1, S2).

The chromatographic peaks of the major fragments in EICs were integrated. The AUC was used to calculate the percentage of the adenosine modifications (Fig. 1A,B).

Deep sequencing library preparation. Deep sequencing libraries were prepared using a combination of three protocols^{12,31,49}.

Chemical fragmentation (metal-ion induced) was used to achieve size distributions of the fragments from 50–200 nt. RNA samples (1–2 µg) were incubated with 100 mM ZnCl₂ in 100 mM Tris-HCl buffer at pH 7.4 at 75 °C for 1 min. The reaction was terminated by addition of EDTA at a final concentration of 50 mM. Samples were ethanol precipitated and the size of the RNA fragments was verified by HS RNA Screen Tape[®].

One half of each sample was incubated with alkaline buffer (50 mM Na₂CO₃, 2 mM EDTA, pH 10.4) for 1 h at 60 °C to convert m¹A into m⁶A via Dimroth rearrangement. Samples were purified by RNA Clean & Concentrator columns (Zymo) and analysed on HS RNA Screen Tape[®].

After denaturation of the RNA samples at 90 °C for 30 s, followed by cooling down on ice, dephosphorylation was performed by 0.5 U of FastAP alkaline phosphatase (ThermoFisher Scientific) in dephosphorylation buffer (at a final concentration 100 mM Tris-HCl, pH 7.4, 20 mM MgCl₂, 0.1 mg/mL BSA and 100 mM 2-mercaptoethanol) for 30 min at 37 °C. The whole procedure was repeated, followed by final heat deactivation of the enzyme at 75 °C for 5 min.

A pre-adenylated adaptor was prepared as described previously⁴⁹ (for the sequence see Supplementary Table S6). Ligation at the 3'-end of RNA was performed at 4 °C for 72 h in dephosphorylation buffer, containing in addition, 15% DMSO, 5 µM adenylated 3'-RNA adaptor, 0.5 U/µL T4 RNA ligase (ThermoFisher Scientific) and 1 U/µL T4 RNA ligase 2 truncated (NEB). The reaction was stopped by heating to 75 °C for 15 min. Unligated 3'-adaptor was removed by 5'-Deadenylase (NEB) and Lambda exonuclease (ThermoFisher Scientific). The mixture was ethanol precipitated.

Reverse transcription with SuperScript III (ThermoFisher Scientific, 10 U/µL) was performed in the First-Strand Buffer, containing RT primer (5 µM), dNTP mix (0.5 mM final conc.), DTT (5 mM), BSA (50 µg/µL) in 30 µL reaction mixture for 1 h at 50 °C. RT primer excess was digested by a combination of Lambda exonuclease, Exonuclease 1 and FastAP alkaline phosphatase (all ThermoFisher Scientific) after reaction. RNA was degraded by NaOH and samples were ethanol precipitated.

Reverse transcription with TGIRT[™]-III (InGex, 1 µL, 500 nM) was performed in 19 µL of reaction buffer (450 mM NaCl, 5 mM MgCl₂, 20 mM Tris-HCl, pH 7.5), with DTT (5 mM) and RT primer (5 µM) for 30 min at room temperature. After 30 min dNTPs (1.25 mM each, final volume 20 µL) were added and the reaction was incubated at 60 °C for 50 min. The reaction was stopped by the addition of 1 µL of 5 M NaOH and was incubated for 3 min at 95 °C. Samples were cooled down at room temperature, neutralized with 1 µL of 5 mM HCl and ethanol precipitated.

3'-Tailing of cDNA was performed using 1 U/µL of Deoxynucleotidyl transferase (TdT, ThermoFisher Scientific) in 1x TdT buffer containing 1.25 mM CTP for 30 min at 37 °C with heat deactivation (75 °C, 10 min). Double stranded DNA anchor was prepared as described previously⁴⁹. Ligation of dsDNA adaptor (1.25 µM) was done in 50 mM Tris-HCl buffer (pH 7.4), containing 10 µM ATP and 20 mM MgCl₂ with T4 DNA ligase (1.5 U/µL) at 4 °C for 72 h. The enzyme was heat deactivated at 65 °C for 10 min. Samples were ethanol precipitated and dissolved in 12 µL of water (molecular biology grade).

PCR amplification was performed with barcoded PCR primers (Supplementary Table S6) in 38 cycles in ThermoPol reaction buffer 1 × (NEB), with 5 µM of each barcoded primer, 0.5 mM dNTPs (each) and 0.25 U of *Taq* DNA Polymerase (NEB) in 20 µL of total reaction mixture. Initial denaturation was performed at 95 °C for 60 s, following by annealing for 60 s at 54 °C, elongation for 60 s at 68 °C and denaturation for 30 s at 95 °C. Final extension was performed at 68 °C for 5 min.

PCR reaction mixture was loaded on 1.3% agarose gel (140 V for 2 h). Fractions between 100–400 nt were cut and DNA was extracted from the gel by NucleoSpin[®] Gel and PCR Clean-up (Macherey –Nagel).

Bioinformatics. Libraries were trimmed using cutadapt⁵⁰ and Atropos⁵¹. Clean sequences longer than 20 bp were mapped to human genome and HIV-1 genome using bwa aligner v0.7.10-r789⁵². All statistics and graphs were generated by custom scripts (github:).

RNA detection by Northern blotting. Isolated RNA from HIV-1 particles and total RNA isolated from infected MT4 cells were each divided in two parts. One part was chemically fragmented as described for the deep sequencing libraries. Denaturing acrylamide gel (20%, 8 × 10 cm; 1 mm thickness) was prepared from 19:1 acrylamide:bis-acrylamide in 0.5x MOPS buffer (10x MOPS buffer stock containing 0.2 M MOPS pH 7.0, 50 mM NaOAc and 10 mM EDTA) and 7 M urea. The polymerized gel was pre-run at 100 V for 30 min in 0.5x MOPS buffer. 15 µL of the RNA samples (400–600 ng of RNA/sample, containing 7.3% formaldehyde, 50% formamide, 0.5x MOPS buffer and 0.01% bromphenol blue) were denatured for 15 min at 55 °C and loaded into the gel wells. The gel was initially run at 50 V for approximately 15 min to concentrate the samples in wells, and then at 150 V until the bromphenol blue reached 90% of the gel length. The gel was blotted onto a charged nylon membrane (Amersham Hybond-N +; GE Healthcare) by capillary transfer in 20x SSC buffer (3 M NaCl, 0.3 M tri-sodium citrate, pH adjusted to 7.0) overnight. The membrane was crosslinked twice on a default setting (120 mJ, 30 s) using electronic ultraviolet crosslinker (Ultralum). The crosslinked membrane was hybridized with 10 mL of Church buffer (70 mM NaH₂PO₄, 180 mM Na₂HPO₄, 7% SDS, 1% BSA, 1 mM EDTA, pH 7.2) at 45 °C for 1 h using a ProBlot hybridization oven (Labnet). Meanwhile, 5 µL of 100 µM probe (Sigma-Aldrich) was end-labelled using 20 U of T4 polynucleotide kinase (NEB), 2 µL of γ-³²P-ATP (3.3 µM, 10 µCi/µL; Hartmann analytic) in 20 µL of supplemented kinase buffer. The labelling was performed at 37 °C for 30 min. The enzyme was inactivated at 65 °C for 5 min and the probe was purified from unincorporated nucleotides using Micro Bio-Spin P-30

columns (BioRad) according to the manufacturer's instructions. The probe was added to the membrane in 10 mL of fresh Church buffer and hybridized at 45 °C overnight. The probe was washed twice for 10 min each with low stringency buffer (2x SSC + 0.1% SDS) and once with high stringency buffer (0.1x SSC + 0.1% SDS), all at 45 °C. The membrane was sealed in foil, incubated with phosphor imaging plate (GE healthcare) and read using Typhoon FLA 9500 (GE Healthcare).

Data Availability

Data from this manuscript is available upon request from the authors.

References

- Helm, M. & Alfonzo, J. D. Posttranscriptional RNA Modifications: Playing Metabolic Games in a Cell's Chemical Legoland. *Chemistry & Biology* **21**, 174–185, <https://doi.org/10.1016/j.chembiol.2013.10.015> (2014).
- Helm, M. & Motorin, Y. Detecting RNA modifications in the epitranscriptome: predict and validate. *Nature Reviews Genetics* **18**, 275, <https://doi.org/10.1038/nrg.2016.169> (2017).
- Carlile, T. M. *et al.* Pseudouridine profiling reveals regulated mRNA pseudouridylation in yeast and human cells. *Nature* **515**, 143, <https://doi.org/10.1038/nature13802>, <https://www.nature.com/articles/nature13802#supplementary-information> (2014).
- Schwartz, S. *et al.* Transcriptome-wide Mapping Reveals Widespread Dynamic-Regulated Pseudouridylation of ncRNA and mRNA. *Cell* **159**, 148–162, <https://doi.org/10.1016/j.cell.2014.08.028> (2014).
- Squires, J. E. *et al.* Widespread occurrence of 5-methylcytosine in human coding and non-coding RNA. *Nucleic Acids Research* **40**, 5023–5033, <https://doi.org/10.1093/nar/gks144> (2012).
- Sakurai, M., Yano, T., Kawabata, H., Ueda, H. & Suzuki, T. Inosine cyanoethylation identifies A-to-I RNA editing sites in the human transcriptome. *Nature Chemical Biology* **6**, 733, <https://doi.org/10.1038/nchembio.434>, <https://www.nature.com/articles/nchembio.434#supplementary-information> (2010).
- Cahová, H., Winz, M.-L., Höfer, K., Nübel, G. & Jäschke, A. NAD captureSeq indicates NAD as a bacterial cap for a subset of regulatory RNAs. *Nature* **519**, 374, <https://doi.org/10.1038/nature14020>, <https://www.nature.com/articles/nature14020#supplementary-information> (2014).
- Walters, R. W. *et al.* Identification of NAD⁺ capped mRNAs in *Saccharomyces cerevisiae*. *Proc. Natl. Acad. Sci. USA* **114**, 480–485, <https://doi.org/10.1073/pnas.1619369114> (2017).
- Jiao, X. *et al.* 5' End Nicotinamide Adenine Dinucleotide Cap in Human Cells Promotes RNA Decay through DXO-Mediated deNADding. *Cell* **168**, 1015–1027, <https://doi.org/10.1016/j.cell.2017.02.019> (2017).
- Dominissini, D. *et al.* Topology of the human and mouse m6A RNA methylomes revealed by m6A-seq. *Nature* **485**, 201, <https://doi.org/10.1038/nature11112>, <https://www.nature.com/articles/nature11112#supplementary-information> (2012).
- Meyer, K. D. *et al.* Comprehensive Analysis of mRNA Methylation Reveals Enrichment in 3' UTRs and near Stop Codons. *Cell* **149**, 1635–1646, <https://doi.org/10.1016/j.cell.2012.05.003> (2012).
- Dominissini, D. *et al.* The dynamic N1-methyladenosine methylome in eukaryotic messenger RNA. *Nature* **530**, 441, <https://doi.org/10.1038/nature16998>, <https://www.nature.com/articles/nature16998#supplementary-information> (2016).
- Zhang, C., Jia, G. & Reversible, R. N. A. Modification N1-methyladenosine (m1A) in mRNA and tRNA. *Genomics, Proteomics & Bioinformatics* **16**, 155–161, <https://doi.org/10.1016/j.gpb.2018.03.003> (2018).
- Safra, M. *et al.* The m1A landscape on cytosolic and mitochondrial mRNA at single-base resolution. *Nature* **551**, 251, <https://doi.org/10.1038/nature24456>, <https://www.nature.com/articles/nature24456#supplementary-information> (2017).
- Gokhale, N. S. *et al.* N6-Methyladenosine in Flaviviridae Viral RNA Genomes Regulates Infection. *Cell Host & Microbe* **20**, 654–665, <https://doi.org/10.1016/j.chom.2016.09.015> (2016).
- Kennedy, E. M. *et al.* Posttranscriptional m6A Editing of HIV-1 mRNAs Enhances Viral Gene Expression. *Cell Host & Microbe* **19**, 675–685, <https://doi.org/10.1016/j.chom.2016.04.002> (2016).
- Keene, S. E., King, S. R. & Telesnitsky, A. 7SL RNA Is Retained in HIV-1 Minimal Virus-Like Particles as an S-Domain Fragment. *Journal of Virology* **84**, 9070–9077, <https://doi.org/10.1128/jvi.00714-10> (2010).
- Telesnitsky, A. & Wolin, S. The Host RNAs in Retroviral Particles. *Viruses* **8**, 235 (2016).
- Larsen, K. P. *et al.* Architecture of an HIV-1 reverse transcriptase initiation complex. *Nature* **557**, 118–122, <https://doi.org/10.1038/s41586-018-0055-9> (2018).
- Zhang, Z., Yu, Q., Kang, S.-M., Buescher, J. & Morrow, C. D. Preferential Completion of Human Immunodeficiency Virus Type 1 Proviruses Initiated with tRNA³ Lys rather than tRNA^{1,2} Lys. *Journal of Virology* **72**, 5464–5471 (1998).
- Auxilien, S., Keith, G., Le Grice, S. F. J. & Darlix, J.-L. Role of Post-transcriptional Modifications of Primer tRNA^{Lys,3} in the Fidelity and Efficacy of Plus Strand DNA Transfer during HIV-1 Reverse Transcription. *Journal of Biological Chemistry* **274**, 4412–4420, <https://doi.org/10.1074/jbc.274.7.4412> (1999).
- Kleiman, L., Jones, C. P. & Musier-Forsyth, K. Formation of the tRNA^{Lys} packaging complex in HIV-1. *FEBS Letters* **584**, 359–365, <https://doi.org/10.1016/j.febslet.2009.11.038> (2010).
- Bilbille, Y. *et al.* The structure of the human tRNA^{Lys3} anticodon bound to the HIV genome is stabilized by modified nucleosides and adjacent mismatch base pairs. *Nucleic Acids Research* **37**, 3342–3353, <https://doi.org/10.1093/nar/gkp187> (2009).
- Eckwahl, M. J. *et al.* Analysis of the human immunodeficiency virus-1 RNA packageome. *RNA*. <https://doi.org/10.1261/rna.057299.116> (2016).
- Eckwahl, M. J., Sim, S., Smith, D., Telesnitsky, A. & Wolin, S. L. A retrovirus packages nascent host noncoding RNAs from a novel surveillance pathway. *Genes & Development* **29**, 646–657, <https://doi.org/10.1101/gad.258731.115> (2015).
- Schopman, N. C. T. *et al.* Selective packaging of cellular miRNAs in HIV-1 particles. *Virus Research* **169**, 438–447, <https://doi.org/10.1016/j.virusres.2012.06.017> (2012).
- Eckwahl, M. J., Telesnitsky, A. & Wolin, S. L. Host RNA Packaging by Retroviruses: A Newly Synthesized Story. *mBio* **7**, <https://doi.org/10.1128/mBio.02025-15> (2016).
- Berkowitz, R., Fisher, J. & Goff, S. P. In *Morphogenesis and Maturation of Retroviruses* (ed Hans-Georg Kräusslich) 177–218 (Springer Berlin Heidelberg, 1996).
- Bagiński, B. *et al.* MODOMICS: a database of RNA modification pathways. 2017 update. *Nucleic Acids Research* **46**, D303–D307, <https://doi.org/10.1093/nar/gkx1030> (2017).
- Hauenschild, R. *et al.* The reverse transcription signature of N-1-methyladenosine in RNA-Seq is sequence dependent. *Nucleic Acids Research* **43**, 9950–9964, <https://doi.org/10.1093/nar/gkv895> (2015).
- Tserovski, L. *et al.* High-throughput sequencing for 1-methyladenosine (m1A) mapping in RNA. *Methods* **107**, 110–121, <https://doi.org/10.1016/j.jymeth.2016.02.012> (2016).
- Kietrys, A. M., Velema, W. A. & Kool, E. T. Fingerprints of Modified RNA Bases from Deep Sequencing Profiles. *Journal of the American Chemical Society* **139**, 17074–17081, <https://doi.org/10.1021/jacs.7b07914> (2017).
- Oerum, S., Dégut, C., Barraud, P. & Tisné, C. m1A Post-Transcriptional Modification in tRNAs. *Biomolecules* **7**, 20 (2017).
- Roovers, M. *et al.* A primordial RNA modification enzyme: the case of tRNA (m1A) methyltransferase. *Nucleic Acids Research* **32**, 465–476, <https://doi.org/10.1093/nar/gkh191> (2004).

35. Narayanan, A. *et al.* Exosomes Derived from HIV-1-infected Cells Contain Trans-activation Response Element RNA. *Journal of Biological Chemistry* **288**, 20014–20033, <https://doi.org/10.1074/jbc.M112.438895> (2013).
36. Wei, F.-Y. *et al.* Deficit of tRNA^{Lys} modification by Cdk11 causes the development of type 2 diabetes in mice. *The Journal of Clinical Investigation* **121**, 3598–3608, <https://doi.org/10.1172/JCI58056> (2011).
37. Jiang, M. *et al.* Identification of tRNAs incorporated into wild-type and mutant human immunodeficiency virus type 1. *Journal of Virology* **67**, 3246–3253 (1993).
38. Mak, J. *et al.* Role of Pr160gag-pol in mediating the selective incorporation of tRNA(Lys) into human immunodeficiency virus type 1 particles. *Journal of Virology* **68**, 2065–2072 (1994).
39. Pavon-Eternod, M., Wei, M., Pan, T. & Kleiman, L. Profiling non-lysyl tRNAs in HIV-1. *RNA* **16**, 267–273, <https://doi.org/10.1261/rna.1928110> (2010).
40. Onafuwa-Nuga, A. A., Telesnitsky, A. & King, S. R. 7SL RNA, but not the 54-kd signal recognition particle protein, is an abundant component of both infectious HIV-1 and minimal virus-like particles. *RNA* **12**, 542–546, <https://doi.org/10.1261/rna.2306306> (2006).
41. McIntyre, W. *et al.* Positive-sense RNA viruses reveal the complexity and dynamics of the cellular and viral epitranscriptomes during infection. *Nucleic Acids Research* **46**, 5776–5791, <https://doi.org/10.1093/nar/gky029> (2018).
42. Yeung, M. L. *et al.* Pyrosequencing of small non-coding RNAs in HIV-1 infected cells: evidence for the processing of a viral-cellular double-stranded RNA hybrid. *Nucleic Acids Research* **37**, 6575–6586, <https://doi.org/10.1093/nar/gkp707> (2009).
43. Schopman, N. C. T. *et al.* Deep sequencing of virus-infected cells reveals HIV-encoded small RNAs. *Nucleic Acids Research* **40**, 414–427, <https://doi.org/10.1093/nar/gkr719> (2012).
44. Kutluay, S. B. *et al.* Global Changes in the RNA Binding Specificity of HIV-1 Gag Regulate Virion Genesis. *Cell* **159**, 1096–1109, <https://doi.org/10.1016/j.cell.2014.09.057> (2014).
45. Zaitseva, L., Myers, R. & Fassati, A. tRNAs Promote Nuclear Import of HIV-1 Intracellular Reverse Transcription Complexes. *PLOS Biology* **4**, e332, <https://doi.org/10.1371/journal.pbio.0040332> (2006).
46. Li, M. *et al.* Codon-usage-based inhibition of HIV protein synthesis by human schlafen 11. *Nature* **491**, 125, <https://doi.org/10.1038/nature11433>, <https://www.nature.com/articles/nature11433#supplementary-information> (2012).
47. Reed, L. J. & Muench, H. A simple method of estimating fifty per cent endpoints¹². *American Journal of Epidemiology* **27**, 493–497, <https://doi.org/10.1093/oxfordjournals.aje.a118408> (1938).
48. Su, D. *et al.* Quantitative analysis of ribonucleoside modifications in tRNA by HPLC-coupled mass spectrometry. *Nature Protocols* **9**, 828, <https://doi.org/10.1038/nprot.2014.047> (2014).
49. Winz, M.-L. *et al.* Capture and sequencing of NAD-capped RNA sequences with NAD captureSeq. *Nature Protocols* **12**, 122, <https://doi.org/10.1038/nprot.2016.163>, <https://www.nature.com/articles/nprot.2016.163#supplementary-information> (2016).
50. Martin, M. Cutadapt removes adapter sequences from high-throughput sequencing reads. *2011 17*, 3, <https://doi.org/10.14806/ej.17.1.200> (2011).
51. Didion, J. P., Martin, M. & Collins, F. S. Atropos: specific, sensitive, and speedy trimming of sequencing reads. *PeerJ* **5**, e3720, <https://doi.org/10.7717/peerj.3720> (2017).
52. Li, H. & Durbin, R. Fast and accurate short read alignment with Burrows–Wheeler transform. *Bioinformatics* **25**, 1754–1760, <https://doi.org/10.1093/bioinformatics/btp324> (2009).

Acknowledgements

We are grateful to Dr. J. Kozák for radioactive labelling of probes for northern blot analysis. This work was supported by the Ministry of Education, Youth and Sports (Czech Republic), programme ERC CZ (LL1603). Funding for open access charge: Ministry of Education, Youth and Sports. The bioinformatics part of the work including access to computing and storage facilities was supported by the ELIXIR CZ research infrastructure project (MEYS Grant No: LM2015047).

Author Contributions

A.S. and H.C. conceived the study. A.S., M.H., M.P., J.H. and H.C. designed the experiments. A.S., B.S., J.T. and M.Z. performed the experiments. J.W., J.C., J.P. and H.C. supervised the work. O.M. and J.P. analysed bioinformatics data. A.S., B.S., J.T. and H.C. wrote the paper.

Additional Information

Supplementary information accompanies this paper at <https://doi.org/10.1038/s41598-019-45079-1>.

Competing Interests: The authors declare no competing interests.

Publisher's note: Springer Nature remains neutral with regard to jurisdictional claims in published maps and institutional affiliations.



Open Access This article is licensed under a Creative Commons Attribution 4.0 International License, which permits use, sharing, adaptation, distribution and reproduction in any medium or format, as long as you give appropriate credit to the original author(s) and the source, provide a link to the Creative Commons license, and indicate if changes were made. The images or other third party material in this article are included in the article's Creative Commons license, unless indicated otherwise in a credit line to the material. If material is not included in the article's Creative Commons license and your intended use is not permitted by statutory regulation or exceeds the permitted use, you will need to obtain permission directly from the copyright holder. To view a copy of this license, visit <http://creativecommons.org/licenses/by/4.0/>.

© The Author(s) 2019